Journal of Physics: Conference Series **688** (2016) 012119 doi:10.1088/1742-6596/688/1/012119

Shock Formation by Plasma Filaments of Microwave Discharge under Atmospheric Pressure

Masayuki Takahashi and Naofumi Ohnishi
Department of Aerospace Engineering, Tohoku University, Japan
E-mail: mtakahashi@rhd.mech.tohoku.ac.jp

Abstract. A one-dimensional compressible fluid calculation was coupled with a finite-difference time-domain code and a particle-in-cell code with collision to reproduce propagation of electromagnetic wave, ionization process of plasma, and shock wave formation in atmospheric microwave discharge. Plasma filaments are driven toward the microwave source at 1 atm, and the distance between each filament is one-fifth of the wavelength of the incident microwave. The strong shock wave is generated due to the high plasma density at the atmospheric pressure. A simple analysis of the microwave propagation into the plasma shows that cut-off density of the microwave becomes smaller with the pressure decrease in a collisional plasma. At the lower pressure, the smaller density plasma is obtained with a diffusive pattern because of the smaller cut-off density and the larger diffusion effect. In contrast with the 1-atm case, the weak shock wave is generated at a rarefied condition, which lowers performance of microwave thruster.

1. Introduction

Significant advancement for space transportation is needed to utilize an outer space as academic study, space travel, military defense, weather observation and so on. Recently, microwave propulsion system has been investigated to launch a small satellite with saving operation cost by high-power energy transmission from a microwave oscillator established on a ground. The irradiated microwave is focused by a parabolic mirror installed on the vehicle, and the intense microwave generates a plasma with sustaining a strong shock wave which supplies an impulsive thrust through interactions with the rocket thruster. In past experiments of the plasma formation by the microwave [1–3], filamentary arrays of the plasma were observed in contrast with a bulk plasma obtained in a laser breakdown [4]. The plasma filaments propagate toward the microwave source at km/s-order velocity, and the distance between each filament is about one-quarter of the incident microwave wavelength. However, at the lower pressure, the plasma cannot form the filamentary structure, and the measured impulse of the microwave rocket drastically drops down [2, 3]. Detailed mechanism of the thrust decrease is not identified by the past experiments; therefore, the plasma and shock generations by the microwave discharge should be examined.

In this study, we have developed a one-dimensional integrated simulator by combining a finite-difference time-domain (FDTD) code, a particle-in-cell with Monte Calro collision (PIC-MCC) code, and a computational fluid dynamics (CFD) code to assess the shock wave and plasma formations by the microwave discharge. We then numerically assess the ambient pressure effects for the plasma and shock wave structures, and specify the mechanism of the thrust decrease at the lower pressure.

2. Numerical Methods

2.1. Interaction between electromagnetic field and plasma

The Maxwell equations are solved by the FDTD method for simulating the microwave propagation. The PIC-MCC method is employed to reproduce the plasma generation in the microwave discharge. In the PIC module, the equation of motion for the charged particles is integrated to examine the interaction between the charged particles and the electromagnetic field assessed by the FDTD simulation. The current density is calculated on the PIC module, and it is fed back to the FDTD module. Also, in the MCC module with a reactive system of N_2, N_2^+, N_2^*, N, e^-, the electron-neutral elastic collision, the electron impact ionization, the electron impact excitation to the first excited state, the neutral dissociation, and the ion-neutral elastic collision processes are considered for a pure nitrogen gas.

2.2. Shock wave calculation

Because the strong shock wave is induced by the microwave discharge, it is necessary to assess the shock wave propagation by coupling the compressible fluid calculation with the plasma simulation. An energy absorption rate by the plasma is estimated from the PIC-MCC simulation, and the absorbed energy is deposited as a source term of a one-dimensional Euler equation to drive the shock wave. For solving the Euler equation, a discretization is performed by a cell-centered finite volume manner. The AUSM-DV method [5] is employed for the numerical flux with the second-order MUSCL method. The temporal integration is done by the first-order Euler explicit method.

3. Simulation Condition

The initial plasma spot which has the Gaussian distribution is set on a computational domain for supposing the first gas breakdown, and the microwave is irradiated from the left boundary to reproduce the microwave-plasma interaction simply. The maximum electric field intensity is 5 MV/m, the microwave frequency is 110 GHz. The simulation domain has the length of 5λ (λ is the microwave wavelength), and the number of grid points is 600.

4. Results and Discussions

4.1. Plasma structures at 1 atm and 0.006 atm

At 1 atm, the plasma filaments are obtained by the microwave incident, and the distance between each filament is about $\lambda/5$, showing well agreement with the experimental and numerical studies [1–3, 6–8] (Fig. 1(a)). The incident microwave is reflected by a over-critical plasma (a critical density of a collisionless plasma: $n_c = 1.5 \times 10^{14}$ cm^3), and the reflected wave generates the quasi-standing wave in front of the plasma, which causes the discrete structure of the plasma filaments (Fig. 1(b)). On the other hand, the clear structure is not obtained at 0.006 atm because of the larger diffusion effect of the electron due to the lower ambient pressure. At 0.006 atm, the maximum density of the plasma becomes smaller than the atmospheric case because the microwave screening density of the plasma decreases with pressure dropping unlike the collisionless plasma in which the critical density is constant. In addition, for the lower pressure, the propagation speed of the plasma front becomes larger than the 1-atm case due to the larger diffusion effect. The estimated propagation speed is order of 1000 km/s at 0.006 atm, while the propagation speed is assessed as order of 10 km/s at 1 atm.

4.2. Analytical prediction of cut-off density

The microwave cannot penetrate into the plasma slab if the plasma density exceeds the cut-off density, and the number density stops to increase because the ionization reaction is suppressed in the plasma. So, the maximum density of the plasma has a relation with the microwave cut-off

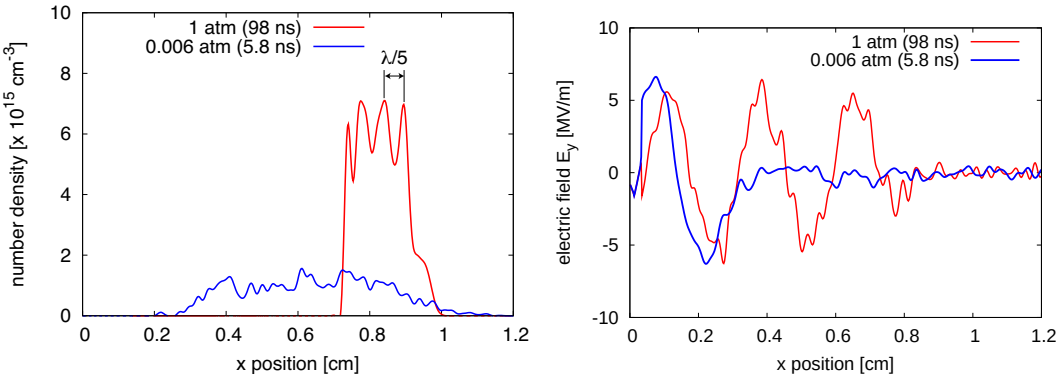

(a) Electron number density (b) Electric field

Figure 1. Electron number density and electric field at 1 atm and 0.006 atm.

density. Because the critical density n_c for the microwave cut-off is given by $n_c = \frac{\epsilon_0 m_e \omega^2}{e^2}$ in the collisionless plasma ($\omega^2 >> \nu_m^2$), there is no pressure dependence for it, where m_e is the electron mass , ω is the incident wave frequency, and e is the elementary charge, ν_m is the elastic collision frequency for electron-neutral collision. However, in the collisional plasma, because the cut-off density changes with the pressure, the maximum density of the plasma slab depends on the ambient pressure. We analytically estimate the cut-off density in the atmospheric plasma to assess the maximum density dependence on the ambient pressure.

For the collisional case, we introduce a wave number to assess the microwave penetration into the plasma. The complex wave number k_x has a dispersion relation in the collisional plasma;

$$k_x = \sqrt{\eta + \xi i}, \tag{1}$$

where i is the imaginary unit, $\eta \equiv \frac{\omega^2}{c^2}(1 - \frac{\omega_p^2}{\omega^2+\nu_m^2})$, and $\zeta \equiv \frac{\omega^2}{c^2}(\frac{\omega_p^2}{\omega^2+\nu_m^2}\frac{\nu_m}{\omega})$ [9]. Equation (1) can be separated to a real part k_{Re} and a imaginary part k_{Im}, that is, $k_{\mathrm{Re}} = \sqrt{\frac{\sqrt{\eta^2+\xi^2}+\eta}{2}}$ and $k_{\mathrm{Im}} = \sqrt{\frac{\sqrt{\eta^2+\xi^2}-\eta}{2}}$. Because the microwave damping by the plasma becomes effective if $k_{\mathrm{Im}} > k_{\mathrm{Re}}$, we obtain the simple relation using the plasma frequency $\omega_p^2 = \frac{ne^2}{\epsilon_0 m_e}$ and the critical density of the collisionless plasma $n_c = \frac{\epsilon_0 m_e \omega^2}{e^2}$;

$$n > \frac{\omega^2 + \nu_m^2}{\omega^2} n_c \equiv n_c'. \tag{2}$$

where n_c' is the cut-off number density for the collisional case. The cut-off density n_c' depends on the ambient pressure p because an elastic collision frequency ν_m is the function of the pressure p. Since the elastic collision frequency ν_m is typically in proportional to the ambient pressure, the cut-off density n_c' decreases with the pressure lowering, which causes the dropping of the maximum density at the rarefied condition.

Figure 2 shows the maximum density estimated by our simulation and the theoretical cut-off density n_c' with the elastic collision frequency of $\nu_m = 5.3 \times 10^9 p$ s^{-1}torr^{-1} [6]. We can obtain a rough agreement for the pressure dependence between the simulation result and the theoretical prediction, but the theoretical line cannot explain a peak at 0.5 atm of our simulation result. The maximum density becomes larger than the cut-off density n_c' because n_c' just indicates that the plasma slab begins to reflect the incident microwave. Detailed analysis is needed to precisely explain the maximum density dependence on the ambient pressure in the microwave discharge.

4.3. Shock wave structures at 1 atm and 0.006 atm

In the microwave propulsion, the shock wave structure induced by the microwave discharge is important for estimating the thrust performance. By combining the FDTD code, the PIC-MCC code, and the CFD code, we can estimate the shock wave structure driven by the intense microwave. At 1 atm, the strong shock wave is generated by the dense plasma due to the larger cut-off density (Fig. 3), resulting in the large thrust in the microwave propulsion. Plateau high pressure remains behind the shock wave like a detonation structure [3] because an energy absorption region at the ionization front moves toward the microwave source with the plasma propagation. On the other hand, at 0.006 atm, the shock wave pressure becomes smaller than the 1-atm case because the plasma density is smaller by the lower cut-off density. This weak shock wave causes the performance dropping of the microwave propulsion at the rarefied condition.

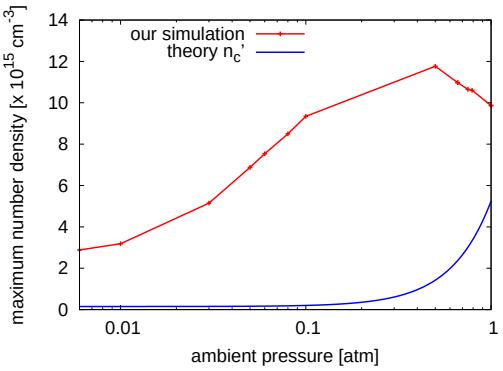

Figure 2. Maximum density calculated by our simulation and theoretical cut-off density.

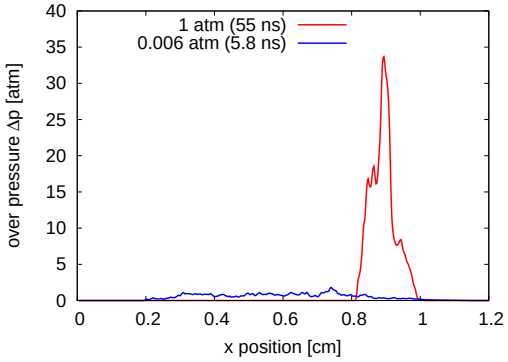

Figure 3. Over pressure profiles at 1 atm and 0.006 atm (over pressure: $\Delta p = p - p_0$, where p is pressure and p_0 is ambient pressure).

5. Conclusion

To simulate the plasma and shock wave formations induced by the microwave discharge, we have developed a coupling simulator constructed by the FDTD module, the PIC-MCC module, and the CFD module. The filamentary arrays are driven toward the microwave source at the atmospheric pressure, and the distance between each filament is one-fifth of the microwave wavelength. Also, the strong shock wave is obtained due to the high plasma density at 1 atm. By a simple estimation of the microwave penetration, we presented that the cut-off density of the collisional plasma becomes smaller with the ambient pressure lowering. At lower pressure, the rarefied and diffusive plasma is obtained because of the smaller cut-off density and the larger diffusion effect. The weak shock wave is generated at the lower pressure, which causes the performance deterioration in the rarefied environment for the microwave propulsion.

References

[1] Hidaka Y. et al. 2008 *Physical Review Letters* **100** 035003.
[2] Oda Y. and Komurasaki K. 2006 *Journal of Applied Physics* **100** 113307.
[3] Oda Y. 2008 *Doctor Thesis*.
[4] Mori K. et al. 2004 *Journal of Applied Physics* **95** (11) 5979–5983.
[5] Wada Y. and Liou M. S. 1994 AIAA Paper 94-0083.
[6] Chaudhury B. et al. 2010 *Physics of Plasmas* **17** 123505.
[7] Boeuf J. P. et al. 2010 *Physical Review Letters* **104** 015002.
[8] Nam K. S. and Verboncoeur P. J. 2009 *: Physical Review Letters* **103** 055004.
[9] Raizer Y. P. 1991 *: Gas Discharge Physics*, Springer publisher.